A Unidirectional DNA Walker Moving Autonomously Along a Track[**]

Peng Yin, Hao Yan*, Xiaoju G. Daniell, Andrew J. Turberfield*, John H. Reif*

[*] Prof H. Yan,

Department of Computer Science, Duke University

Durham, NC 27708, USA

Email: hy1@cs.duke.edu

[*] Prof A. J. Turberfield,

University of Oxford, Department of Physics, Clarendon Laboratory

Parks Road, Oxford OX1 3PU, UK

Email: A.Turberfield@physics.ox.ac.uk

[*] Prof J. H. Reif,

Department of Computer Science, Duke University

Durham, NC 27708, USA

Email: reif@cs.duke.edu

P. Yin, X. G. Daniell,

Department of Computer Science, Duke University

[**] This work was supported by grant from NSF (EIA-0218359) to Hao Yan and John H. Reif, and by NSF ITR Grants EIA-0086015 and CCR-0326157 and DARPA/AFSOR Contract F30602-01-2-0561.

Keywords: DNA, Nanostructures, Nano-robotics, Self-assembly, Autonomous molecular devices

A major challenge in nanotechnology is to precisely transport a nanoscale object from one location on a nanostructure to another location following a designated path. The successful construction of self-assembled DNA nanostructures provides a solid structural foundation to meet this challenge. DNA, with its immense information encoding capacity and well defined Waston-Crick complementarity, has been explored as an excellent building material for nanoconstruction.[1,2] In particular, recent years have seen remarkable success in both the construction of self-assembled nanostructures and individual nanomechanical devices. For example, one and two dimensional DNA lattices have been constructed from a rich set of branched DNA molecules.[3-7] These DNA lattices could provide a platform for embedded DNA nanomechanical devices to perform the desired transportation. A diverse group of DNA nanomechanical devices have also been demonstrated. These include DNA nanodevices executing cycles of motions such as open/close,[8-11] extension/contraction,[12-14] and reversible rotation.[15,16] Such DNA based nanodevices can be cycled between well-defined states by means of external intervention such as sequential addition of DNA 'fuel strands'[8-10,12-14,16] or the change of ionic composition of the solution.[11,15] However, these devices are unsuitable for the above challenge for two reasons. First, they demonstrate only local conformation changes, not progressive motion. Secondly, they do not move autonomously. Various schemes of autonomous DNA walker devices based on DNA cleavage and ligation have been explored theoretically but not experimentally;[17] these were limited to random bidirectional movement. The use of DNA hybridization as an energy source for autonomous molecular motors has also been proposed.[18] Recent papers report the construction of a non-autonomous DNA biped walker device[19] and autonomous DNA tweezers.[20] The production of a DNA motor capable of autonomous, unidirectional, progressive linear translational motion is an important next step in the development of DNA-based molecular devices.

Here we report the design and construction of an autonomous, unidirectional DNA motor that moves along a DNA track. The self-assembled track contains three anchorages at which the walker, a six-nucleotide DNA fragment, can be bound. At each step the walker is ligated to the next anchorage, then cut from the previous one by a restriction endonuclease. Each cut destroys the previous restriction site and each ligation creates a new site in such a way that the walker can not run backwards. The motor is powered by the hydrolysis of adenosine triphosphate (ATP), a kinetically inert fuel whose breakdown may be accelerated by many orders of magnitude by protein catalysts.[21] Operation of the motor was verified by tracking the radioactively labeled walker using gel electrophoresis.

The autonomous, unidirectional, along-the-track motion demonstrated by this prototype system represents a novel type of motion for DNA based nanomechanical devices. The motion of the walker can be extended in principle beyond 3 anchorages. Embedding a walking device of this kind in a DNA lattice would result in a nano-robotics lattice that can meet the challenge stated above: a nanoscale 'walker' that moves autonomously along a designated path over a microscopic structure, serving as a carrier of information and possibly physical cargo such as nanoparticles.

The structural design of the device is shown in Figure 1a (base sequences for all components are given in Figure S1a in Supporting Information). The track consists of three evenly spaced DNA double helical 'anchorages' (A, B, and C), each tethered to another DNA duplex segment which forms part of the backbone of the track by means of a 4-nucleotide 'hinge'. Each anchorage consists of 13 base pairs, with a 3-nucleotide single-strand overhang ('sticky end'). Each anchorage is positioned 3 helical turns (31 or 32 base pairs) away from its nearest neighbours. The duplex segments of the backbone of the track and of the three anchorages are expected to behave like rigid rods since they are much shorter than the persistence length of duplex DNA (greater than 10 turns).[22, 23] In contrast, the 4-nucleotide single-

strand hinge is expected to be flexible, since the persistence length of the single DNA strand is 3 nucleotides.[24] A 6-nucleotide DNA 'walker', labeled * and coloured red, moves sequentially along the track from anchorage A to B, then to C.

The device is constructed by mixing stoichiometrically purified DNA oligonucleotides in hybridization buffer (see Experimental Section) and slowly cooling the system from 90 °C to 37 °C. The solution is then supplemented with T4 ligase, endonuclease PflM I, and endonuclease BstAP I and incubated at 37 °C. Autonomous motion of the walker is initiated by the addition of the energy source, ATP.

The recognition sites and restriction patterns of PflM I and BstAP I are shown in Figure 1b. Figure 1c shows the sequence of structural changes that occur during the motion of the walker; the right portion shows the base sequence at the end of each anchorage at each stage, and how these are transformed by enzyme actions. The motion of the walker depends on alternate enzymatic ligation and restriction (cleavage). Before the motion starts the walker, whose position is indicated by *, resides at anchorage A, as shown in panel 0 of Figure 1c. In this state anchorages A* and B have complementary sticky ends which can hybridize with each other. T4 ligase can then heal the nicks at either end of the newly-hybridized section, covalently joining the two anchorages (A* + B $\rightarrow$ A*B); this is an irreversible step that consumes energy provided by the hydrolysis of ATP. The ligation of A*B creates a recognition site for endonuclease PflM I. In process II, PflM I cleaves A*B in such a way that the walker moves to anchorage B: A*B $\rightarrow$ A + B*. The sticky end of anchorage B* can then hybridize with the complementary sticky end of anchorage C, and the two anchorages are ligated to form B*C in process III. Ligation product B*C contains a recognition site for the second endonuclease BstAP I. In process IV, B*C is cleaved by BstAP I to regenerate anchorage B and create C*. Thus the walker moves from anchorage B to C, completing the autonomous, programmed motion of the walker.

The motion of the walker is unidirectional: the product of ligation between two neighbouring anchorages can only be cleaved such that the walker moves onto the downstream anchorage (A*B and B*C can only be cut such that the walker is left attached to B and C respectively). Two idling steps are possible: B* can be religated to A, and regenerated by restriction by PflM I; similarly C* can be re-ligated to B and regenerated by BstAP I. However, these idling steps neither reverse nor block the overall unidirectional motion of the walker. Once B* has been ligated to C the walker can never return to A.

The autonomous and unidirectional motion of the walker was verified by using denaturing polyacrylamide gel electrophoresis (PAGE) to track the motion of the walker, which was radioactively labeled. The position reached by the walker in the presence of different combinations of enzymes can be determined by measuring the size of the labeled DNA fragment. Figure 2a is a schematic drawing of the experimental design. The 5′ end of the walker (red) was labeled with γ-P^{32}, represented by a red dot in Figure 2a. Initially, the labeled strand (part of A*) measures 52 nucleotides. The completion of processes I, II, III, and IV can be detected by the appearance of radioactively labeled bands of 68, 19, 57, and 41 nucleotides respectively, corresponding to the transfer of the radioactive labeled fragment between the anchorages along the track. The system was incubated at 37 °C in hybridization buffer supplemented with ATP and BSA and in the presence of different combinations of enzymes, which were added to the system simultaneously. Figure 2b is an autoradiograph of a denaturing gel showing the products formed during each reaction. Lane 1 contains the control reaction without enzyme or ATP. Lane 2 contains T4 ligase and ATP: the walker is expected to complete process I to produce a radio-labeled strand of 68 nucleotides corresponding to the formation of A*B. Lane 3 contains both T4 ligase and endonuclease PflM I: the walker is expected to be able to follow the reaction sequence shown in Figure 2a as far as completion of process III. Upon completion of process II, A*B is cut to produce A

and B*, resulting in a labeled strand of 19 nucleotides. Subsequently, B* can be ligated to C to form B*C, giving rise to a strand of 57 nucleotides. (These stages in the motion of the walker were also observed in a time course experiment - see Figure S2 in Supporting Information). Lane 4 contains all three enzymes: the walker is expected to be able to run autonomously to the completion of process IV in which B*C is cleaved by BstAP I to generate C*, producing a labeled strand of 41 nucleotides. The radioactively labeled bands in the gel shown in Figure 2b agree with all the above expectations and hence provide evidence for the designed autonomous, unidirectional motion of the walker.

To further test the operation of the system we forced the device to operate in a stepwise fashion (rather than autonomously) by sequentially adding and deactivating the enzymes. This experiment enabled us to inspect more closely the products formed at the end of each process. The walker was radioactively labeled as described above. Figure 2c is an autoradiograph of a denaturing gel showing the products after each step. The system was first supplemented with T4 ligase: the appearance of a 68-nucleotide DNA band in Lane 2 demonstrates the completion of process I and the formation of A*B. The solution was left at 37 °C for one day to deactivate T4 ligase,[1] then PflM I was added (Lane 3). The band of 68 nucleotides, corresponding to A*B, diminished while a band of 19-nucleotides, corresponding to B*, appeared, which confirms the completion of process II. The system was then incubated at 37 °C for two more days to deactivate PflM I,[2] and was again supplemented with T4 ligase and ATP (Lane 4). The intensity of the 19-nucleotide band, corresponding to B*, dramatically decreased while the intensity of the 68-nucleotide band, corresponding to A*B, increased and a 57-nucleotide band, corresponding to B*C also appeared. This is consistent with our expectation that B* can be ligated to both A and C. Note that the formation of A*B is only an idling step in the motion of the walker. After

[1] The half-life of T4 ligase at 37 °C is approximately 4 hours ("New England Biolabs unpublished observations").
[2] The half-life of PflM I at 37 °C is approximately 16 hours ("New England Biolabs unpublished observations").

the enzyme activity of T4 ligase died out one more day later, the addition of BstAP I resulted in the disappearance of the 57-nucleotide band and the appearance of a 41-nucleotide band indicating the cleavage of B*C to B and C* (Lane 5). Note that the intensity of the 68-nucleotide band was approximately unchanged, which confirms that A*B is resistant to the restriction activity of BstAP I as designed. These measurements provide further confirmation that the device operates as designed.

The unidirectional motion of the walker was also tested by two control experiments depicted in Figure 3. In the first experiment, shown in Figure 3a & b, we intentionally constructed the device such that the walker initially resides at anchorage B. Figure 3a shows the forward and idling processes that we expect to be allowed, and reversing processes that we expect to be forbidden. The 19-nucleotide strand B* was labeled with γ-P^{32} at its 5′ end, indicated by the red dot. Figure 3b shows the products generated by addition of different combinations of restriction enzymes and ligase. In the presence of T4 ligase (Lane 2 of Figure 3b) the appearance of 68- and 57-nucleotide bands indicate the formation of A*B and B*C respectively. Addition of BstAP I (Lane 5), which is designed to cut B*C into B and C*, decreases the intensity of the B*C band and generates the 16-nucleotide fragment B as expected. Addition of PflM I (Lane 4), which is designed to cut A*B into A and B*, decreases the intensity of the A*B band but generates no B, again as expected. Lane 3 shows the case when all three enzymes are present.

In the second control experiment depicted in Figure 3c, d the device was constructed with the walker initially at anchorage C. The 5′ end of the 41-nucleotide strand of anchorage C* was labeled with γ-P^{32}. In the presence of T4 ligase (Lane 2 of Figure 3d) the appearance of a 57-nucleotide band indicates the formation of B*C as expected. Subsequent lanes, corresponding to different combinations of restriction enzymes and ligase, show that B*C can be restricted to B and C* by BstAP I as expected, but that no combination of enzymes leads to the backwards step $B^*C \rightarrow B^* + C$ (which would have

been indicated by a 19-nucleotide labeled band corresponding to B*).

By measuring the intensities of the bands in Figures 2b we have estimated the following yields for steps in the operation of the device: A* → A*B, 46%; A*B → B*C, 51%; B*C→ C*, 97%. Both imprecise stoichiometry and low ligation/cleavage efficiency could cause low measured yields. Low enzymatic efficiencies might be result from the steric constraints imposed by the design of the motor; each substrate is created by hybridization of two anchorages, which are also linked by the backbone of the track. We are currently investigating design improvements including structural modifications such as increasing the length of the linkage between each anchorage and the backbone.

The reactions described in this paper were carried out in solution, where the possibility exists that the anchorages of two individual devices might interact with each other in such a way that the walker of one device might deviate from its designated track and move onto the track of another device. In a control experiment described in Supporting Information we have shown that under conditions corresponding to the measurements described above the linkage of two tracks is undetectable (see Figure S3 in Supporting Information).

In summary, we have designed and constructed a nanoscale device in which an autonomous walker moves unidirectionally along a DNA track, driven by the hydrolysis of ATP. The motion of the walker in principle can be extended well beyond the 3-anchorage system demonstrated here.[25] Discovery of new endonucleases with larger non-specific spacing regions within their recognition sequences could lead to walkers of larger sizes. By encoding information into the walker and the anchorages, the device can be extended into a powerful autonomous computing device (and hence an “intelligent” robotics device). [26]

Experimental Section:

DNA sequences were designed and optimized with the SEQUIN software[27] and are listed in Figure S1 in Supporting Information. DNA strands were commercially synthesized by Integrated DNA Technology, Inc. (www.idtdna.com) and purified by denaturing gel electrophoresis. The concentrations of DNA strands were determined by measurement of ultraviolet absorption at 260 nm. To assemble the track, DNA strands were mixed stoichiometrically at 0.3 μM in hybridization buffer and incubated in a heating block from 90 °C to 37 °C over a period of 3 hours. We use NEB 3 buffer purchased from New England Biolabs (www.neb.com) as the hybridization buffer: NEB 3 contains 100 mM NaCl, 50 mM Tris-HCl, 10 mM $MgCl_2$, and 1mM dithiothreitol (pH 7.7 at 37 °C). For radioactive labeling of DNA strands, DNA strands were labeled with T4 polynucleotide kinase purchased from Invitrogen Inc. (www.invitrogen.com), using the standard protocol recommended by the kinase kit. For the ligation and endonuclease cleavage experiments, 30 μl solution containing 1 picomole of assembled device was supplemented with BSA and ATP such that it contained 100 μg/ml BSA and 1 mM ATP. 1 unit of T4 Ligase, 24 units of endonuclease PflM I, and 5 units of endonuclease BstAP I were added to the solution, followed by overnight incubation at 37 °C. Endonucleases PflM I and BstAP I were purchased from New England Biolabs (www.neb.com). T4 ligase was purchased from Invitrogen Inc. (www.invitrogen.com). The reaction solution was NEB 3 buffer supplemented with BSA and ATP, containing 100 mM NaCl, 50 mM Tris-HCl, 10 mM $MgCl_2$, 1 mM dithiothreitol (pH 7.7 at 37 °C), 100 μg/ml BSA, and 1 mM ATP. Enzymatic reactions were carried out at 37 °C. For denaturing gel electrophoresis, the mixture was heated at 90 $^{\circ}$C for 10 minutes, and applied to denaturing polyacrylamide gel. The positions of the radioactively labeled strands were detected via phosphor-imager. The relative concentrations of DNA present in the bands were measured using ImageQuant from Molecular Dynamics (www.mdyn.com).

References

[1] N. C. Seeman, *Nature* **2003**, *421*, 427-431.

[2] C. M. Niemeyer, M. Adler, *Angew. Chem.* **2002**, *114*, 3933-3937, *Angew. Chem. Int. Edit.* **2002**, *41*, 3779-3783.

[3] E. Winfree, F. Liu, L. A. Wenzler, N. C. Seeman, *Nature* **1998**, *394*, 539-544.

[4] C. Mao, W. Sun, N. C. Seeman, *J. Am. Chem. Soc.* **1999**, *121*, 5437-5443.

[5] T. H. LaBean, H. Yan, J. Kopatsch, F. Liu, E. Winfree, J. H. Reif, N. C. Seeman, *J. Am. Chem. Soc.* **2000**, *122***,** 1848-1860.

[6] H. Yan, T. H. LaBean, L. Feng, J. H. Reif, *Proc. Natl. Acad. Sci. U. S. A.* **2003**, *100*, 8103-8108.

[7] H. Yan, S. H. Park, G. Finkelstein, J. H. Reif, T. H. LaBean, *Science* **2003**, *301*, 1882-1884.

[8] B. Yurke, A. J. Turberfield, A. P. Mills Jr, F. C. Simmel, J. L. Neumann, *Nature* **2000**, *406*, 605-608.

[9] F. C. Simmel, B. Yurke, *Phys. Rev. E* **2001**, *63*, 041913.

[10] F. C. Simmel, B. Yurke, *Appl. Phys. Lett.* **2002,** *80*, 883-885.

[11] D. Liu, S. Balasubramanian, *Angew. Chem.* **2003**, *115*, 5912-5914; *Angew. Chem. Intl. Ed.* **2003**, *42*, 5734-5736.

[12] L. Feng, S. H. Park, J. H., Reif, H. Yan, *Angew. Chem.* **2003,** *115*, 4478-4482; *Angew. Chem. Int. Ed.* **2003,** *42*, 4342-4346.

[13] P. Alberti, J-L. Mergny, *Proc. Natl. Acad. Sci. U. S. A.* **2003,** *100*, 1569-1573.

[14] J. J. Li, W. Tan, *Nano Lett.* **2002**, *2*, 315-318.

[15] C. Mao, W. Sun, Z. Shen, N. C. Seeman, *Nature* **1999**, *397*, 144-146.

[16] H. Yan, X. Zhang, Z. Shen, N. C. Seeman, *Nature* **2002**, *415*, 62-65.

[17] J. H. Reif, *Lecture Notes in Computer Science* **2003**, *2568*, 22-37.

[18] A. J. Turberfield, J. C. Mitchell, B. Yurke, A. P. Mills Jr., M. I. Blakey, F. C. Simmel, *Phys. Rev. Lett.* **2003**, *90*, 118102.

[19] W. B. Sherman, N. C. Seeman, *Nano Lett.*, In press (2004).

[20] Y. Chen, M. Wang, C. Mao, *Angew. Chem.* **2004**, *116*, 3638-3641; *Angew. Chem. Int. Ed.* **2004**, *43*, 3554-3557.

[21] F. H. Westheimer, *Science* **1987**, *235*, 1173-1178.

[22] S. B. Smith, L. Finzi, C. Bustamante, *Science* **1992**, *258*, 1122-1126.

[23] G. S. Manning, *Biopolymers* **1981**, *20*, 1751-1755.

[24] S. B. Smith, Y. Cui, C. Bustamante, *Science* **1996**, *271*, 795-799.

[25] P. Yin, A. J. Turberfield, J. H. Reif, "Designs for Autonomous Unidirectional Walking DNA Devices" in *Tenth International Meeting on DNA Computing*, **2004**.

[26] P. Yin, A. J. Turberfield, S. Sahu, J. H. Reif, "Design for an Autonomous DNA Nanomechanical Device Capable of Universal Computation and Universal Translational Motion" in *Tenth International Meeting on DNA Computing*, **2004**.

[27] N. C. Seeman, *J. Biomol. Struct. Dyn.* **1990**, *8*, 573-581.

Figure Legends:

Figure 1. The structural design and operation of the autonomous unidirectional device. **a).** Structural design. The device contains two parts: the track and the walker. The track consists of three evenly spaced duplex DNA anchorages, A, B, and C, each linked to the backbone via a hinge, a 4-nucleotide flexible single-stranded DNA fragment. The walker is a 6-nucleotide DNA fragment (coloured red and indicated by *) initially positioned at anchorage A. The numbers give the lengths of DNA fragments in bases. **b).** Recognition sites and restriction patterns of PflM I and BstAP I. Green (pink) boxes indicate

the recognition site of PflM I (BstAP I) and green (pink) arrows indicate their restriction sites. Bases that are important for PflM I (BstAP I) recognition are shown in bold green (pink) fonts. N indicates the position of a base that does not affect recognition. **c).** Operation of the device. The left portion shows the sequence of structural changes that occur during the device's operation; the right portion describes the accompanying enzyme actions and shows how they affect the ends of the anchorages. Panel 0 depicts the device in its initial state. Process I is the ligation of anchorage A* and anchorage B which have complementary sticky ends; purple curves indicate the ligation sites. Note that ligation of A* with B creates a PflM I recognition site, indicated by green boxes in Panel 1; the cuts made by this enzyme are indicated with two green arrows. In process II, the device is cleaved by PflM I, transferring the walker to anchorage B (Panel 2). The new sticky end of B* is complementary to that of C. In process III, anchorage B* and anchorage C hybridize with each other, and are ligated by T4 ligase to create a recognition site for endonuclease BstAP I. Purple curves in Panel 3 indicate the ligation sites; pink boxes and arrows indicate the BstAP I recognition site and restriction pattern respectively. In process IV, B*C is cleaved into B and C*, transferring the walker to anchorage C. This completes the motion of the walker, and the final product is shown in panel 4.

Figure 2. Evidence of the autonomous unidirectional motion of the walker. **a).** Experimental design. The six-nucleotide walker is coloured red. The red dot indicates the radioactive label; at each stage the radioactively labeled strand is illustrated as a thickened line, with its length in bases shown near its 5′ end. **b).** PAGE analysis of the autonomous motion of the walker. An autoradiograph of a 20% denaturing polyacrylamide gel identifies the position of the radioactively labeled walker. Lane 0: labeled 10 bp DNA ladder marker. Lane 1: device with no enzymes (control). Lanes 2-4: device with T4 ligase, ATP, and different combinations of endonucleases PflM I and BstAP I as indicated. **c).** PAGE analysis

of the stepwise motion of the walker. Lane 0: labeled 10 bp DNA ladder marker. Lane 1: device with no enzymes (control). Lanes 2-5 contain samples corresponding to the stepwise completion of processes I, II, III, and IV in Figure 2a respectively as described in the text. Oligonucleotide lengths (in bases) corresponding to DNA bands are indicated beside the gels.

Figure 3. Control experiments. **a** and **c** show the design of control experiments in which the device is prepared with the walker (coloured red) initially attached to anchorages B and C respectively. Red dots indicate the γ-P^{32} label; the corresponding labeled strand is shown as a thickened line, with its length in bases shown near its 5′ end. A red cross on a broken arrow means the reaction indicated by that arrow is not expected to happen. **b** and **d** are autoradiographs of denaturing 20% PAGE gels showing the results of the experiments indicated in parts **a** and **c** respectively. In both gels, Lane 0 contains a labeled 10 bp DNA ladder marker. Lane 1 contains the device with no enzymes (control). Lanes 2-5: device with T4 ligase, ATP, and different combinations of endonucleases PflM I and BstAP I as indicated. Oligonucleotide lengths (in bases) corresponding to DNA bands are indicated beside the gels.

Suggested Text for the Table of Contents

Autonomous, unidirectional DNA walker moving along a track: The self-assembled track contains three anchorages (A, B, C) at which the walker (*), a six-nucleotide DNA fragment, can be bound. At each step the walker is ligated to the next anchorage, then cut from the previous one by a restriction endonuclease. Each cut destroys the previous restriction site and each ligation creates a new site in such a way that the walker can not run backwards. The walker is powered by the hydrolysis of ATP.

Supporting Information

A Unidirectional DNA Walker Moving Autonomously Along a Track,

by P. Yin, H. Yan, X. G. Daniell, A. J. Turberfield, & J. H. Reif

Supplemental Figure S1. DNA strand structure and sequences. **a)**. Base sequences of the oligonucleotides that make up the molecular device. **b)** and **c)**. Base sequences of the oligonucleotides used to construct the monomer and dimer control molecules described in the caption to Supplemental Figure S3.

Supplemental Figure S2. Time course experiment. Supplemental Figure S2 is an autoradiograph of a 20% denaturing polyacrylamide gel showing the time course of the device's motion under conditions corresponding to Figure 2b Lane 3. Lane 0: 10 bp ladder marker. Lane 1: device with no enzymes (control). Lanes 2-7 contain samples incubated with T4 ligase and PflM I at 37 °C for 15 minutes, 30 minutes, 1 hour, 2 hours, 4 hours, and 8 hours respectively. The monotonic increase in the concentration of the product B*C, and the decrease in the concentration of the intermediate B* after the first 30 minutes, are consistent with the designed unidirectional motion of the walker.

Supplemental Figure S3. Test for inter-molecular reactions. Complexes produced during the operation of the device were analyzed using a native gel to test for the formation of dimers caused by cross-linkage of two devices. **a** and **c** depict the molecular designs of 'monomer' and 'dimer' control complexes. The designs of the controls are shown in Figure S1b and Figure S1c respectively. The control complexes do not have exactly the

same sequences or structures as the corresponding states of the device; they have approximately the same structures and are designed to migrate at approximately the same rates without forming higher multimers. The monomer control corresponds approximately to the state of a single device at the end of process I or III in Figure 1c. The dimer control represents an intermolecular complex formed by ligation of anchorages on different motors. **b).** Autoradiograph of the 8% native polyacrylamide gel used to test for inter-molecular reactions. The assembled device system was incubated at 37 °C in hybridization buffer supplemented with ATP and BSA and in the presence of various combinations of enzymes. Lane 1: labeled monomer control. Lane 2: device with no enzymes (control). Lane 3: device with T4 ligase. Lane 4: device with T4 ligase, endonucleases PflM I and BstAP I. Lane 5: labeled dimer control. No dimer band was detected in Lanes 2-4, indicating the absence of inter-molecular interactions during the operation of the device.

We note that there is a slight displacement between bands in Lanes 1 and 2, and a matching broadening of bands in Lanes 3 and 4. This is consistent with the hypothesis that a device with no linkages between its anchorages (present in Lane 2 and as part of the population in Lanes 3 and 4) migrates slightly more slowly than a device with two anchorages ligated together (control Lane 1 and part of the population in Lanes 3 and 4).

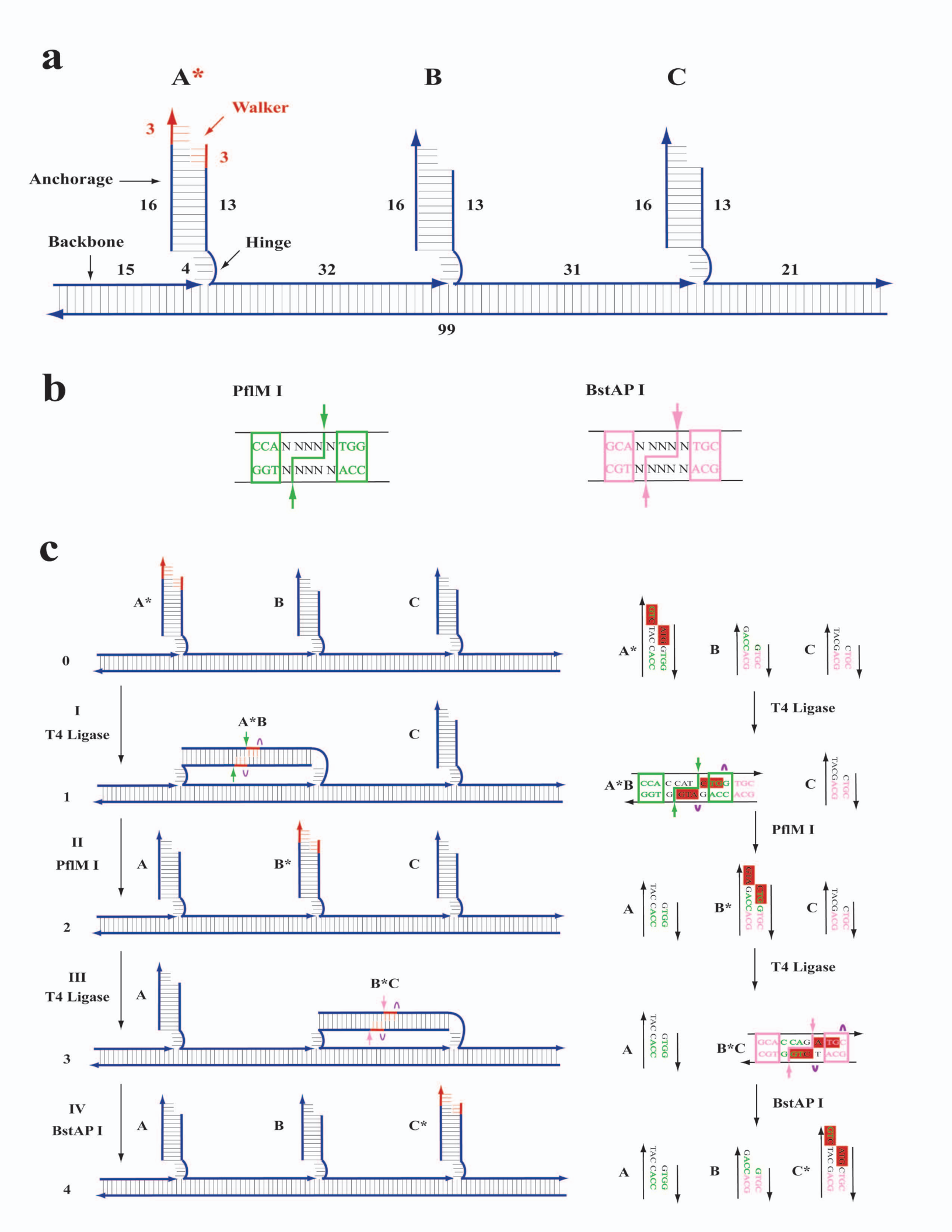
a
A*
B
C
Walker
3
3
Anchorage
16
13
16
13
16
13
Backbone
Hinge
15
4
32
31
21
99
b
PflM I
CCA N NNN N TGG
GGT N NNN N ACC
BstAP I
GCA N NNN N TGC
CGT N NNN N ACG
c
A*
B
C
0
I
T4 Ligase
A*B
C
1
II
PflM I
A
B*
C
2
III
T4 Ligase
A
B*C
3
IV
BstAP I
A
B
C*
4
T4 Ligase
PflM I
T4 Ligase
BstAP I

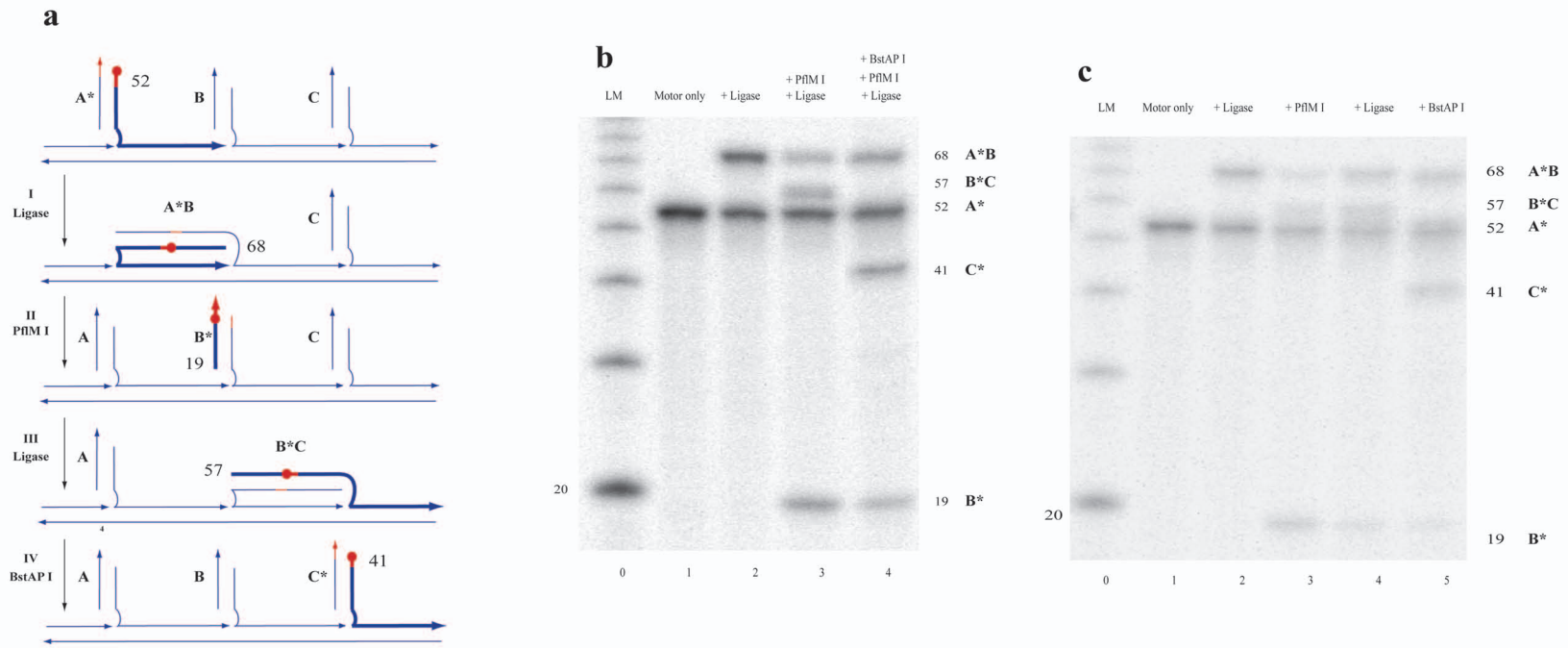
a
A*
52
B
C
I
Ligase
A*B
68
C
II
PflM I
A
B*
19
C
III
Ligase
A
B*C
57
4
IV
BstAP I
A
B
C*
41
b
LM
Motor only
+ Ligase
+ PflM I
+ Ligase
+ BstAP I
+ PflM I
+ Ligase
68 A*B
57 B*C
52 A*
41 C*
20
19 B*
0
1
2
3
4
c
LM
Motor only
+ Ligase
+ PflM I
+ Ligase
+ BstAP I
68 A*B
57 B*C
52 A*
41 C*
20
19 B*
0
1
2
3
4
5

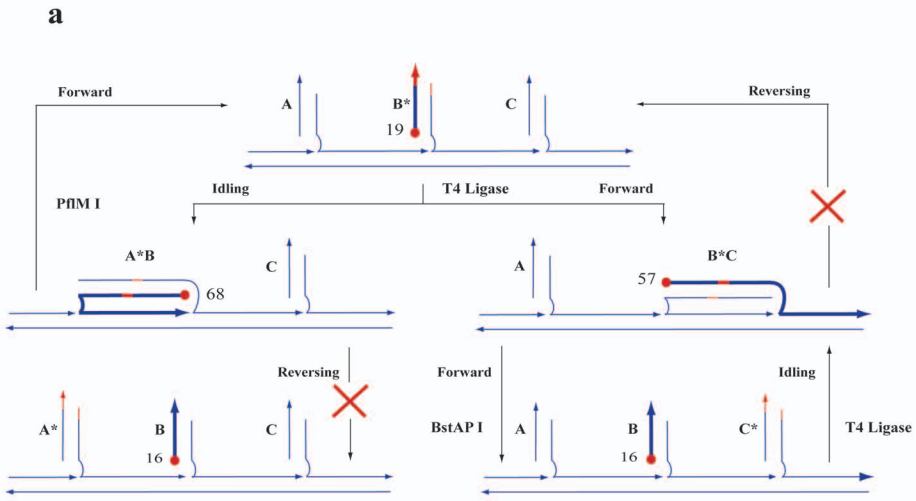
a
Forward
A
B*
19
C
Reversing
PflM I
Idling
T4 Ligase
Forward
A*B
68
C
A
B*C
57
Reversing
Forward
Idling
A*
B
16
C
BstAP I
A
B
16
C*
T4 Ligase

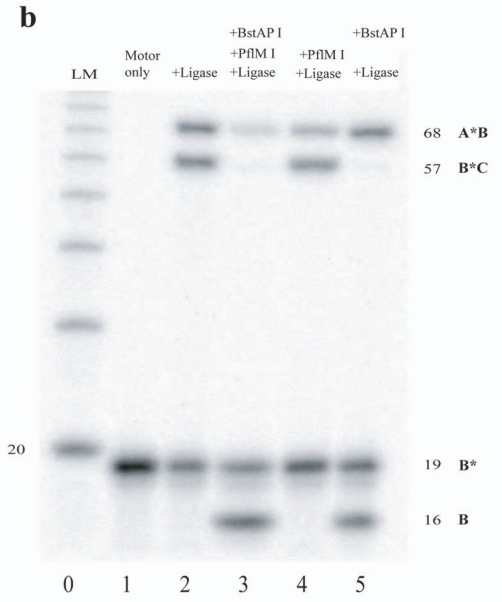
b
LM
Motor only
+Ligase
+BstAP I +PflM I +Ligase
+PflM I +Ligase
+BstAP I +Ligase
68 A*B
57 B*C
20
19 B*
16 B
0 1 2 3 4 5

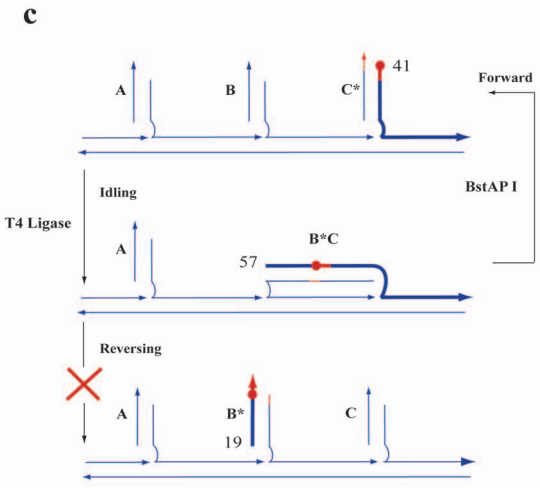
c
A
B
C*
41
Forward
BstAP I
Idling
T4 Ligase
A
B*C
57
Reversing
A
B*
19
C

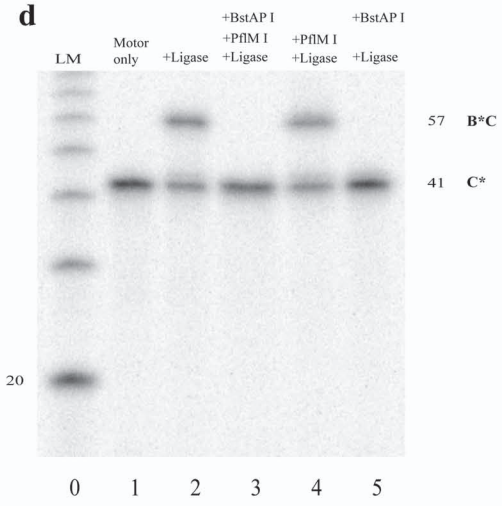
d
LM
Motor only
+Ligase
+BstAP I +PflM I +Ligase
+PflM I +Ligase
+BstAP I +Ligase
57 B*C
41 C*
20
0 1 2 3 4 5

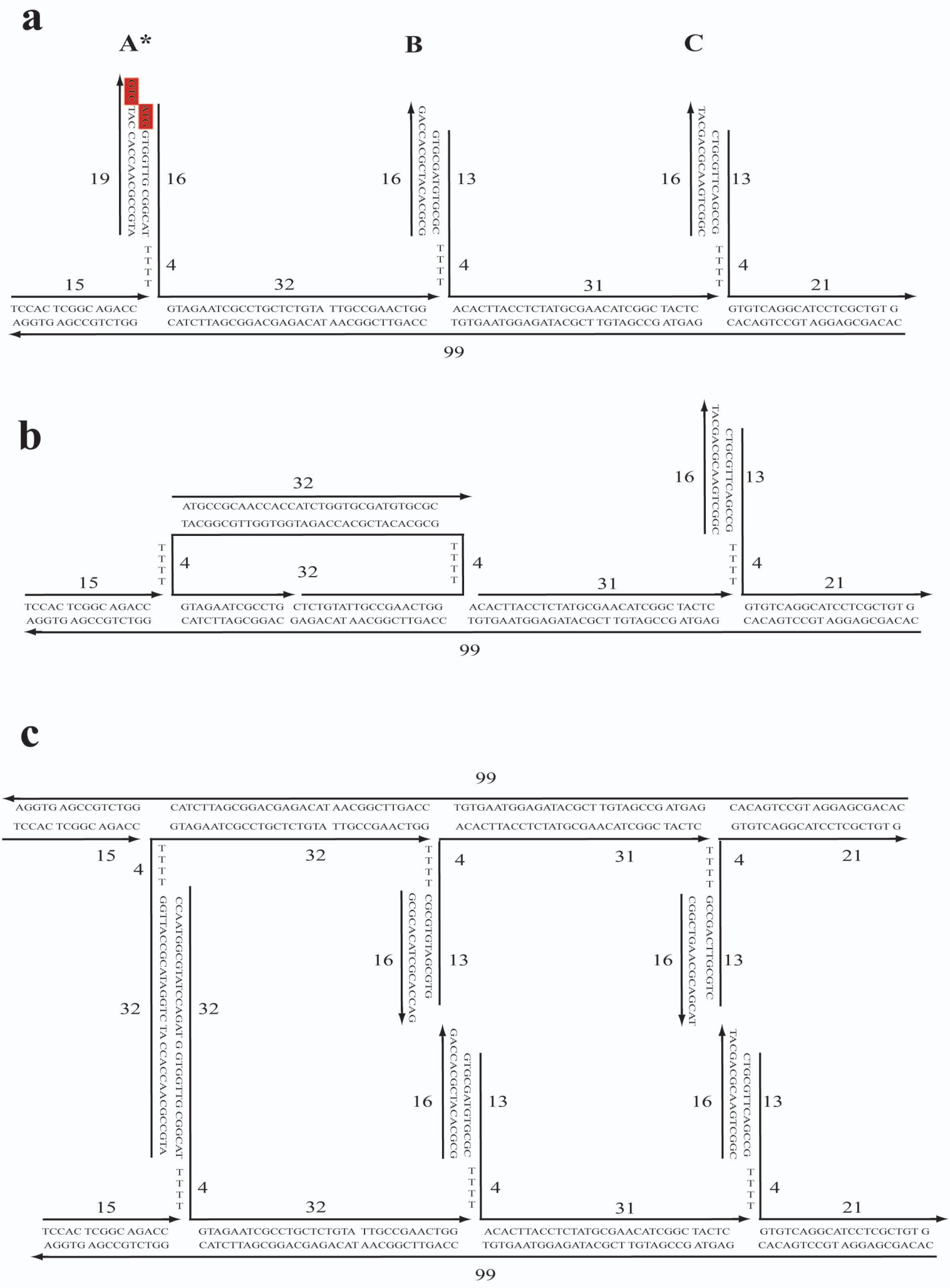
a
A*
B
C
GTC
ATG
TAC CACCAACGCCGTA
GTGGTTG CGGCAT
19
16
4
15
32
31
21
GACCACGCTACACGCG
GTGCGATGTGCGC
16
13
4
TACGACGCAAGTCGGC
CTGCGTTCAGCCG
16
13
4
TCCAC TCGGC AGACC
AGGTG AGCCGTCTGG
GTAGAATCGCCTGCTCTGTA TTGCCGAACTGG
CATCTTAGCGGACGAGACAT AACGGCTTGACC
ACACTTACCTCTATGCGAACATCGGC TACTC
TGTGAATGGAGATACGCT TGTAGCCG ATGAG
GTGTCAGGCATCCTCGCTGT G
CACAGTCCGT AGGAGCGACAC
99
b
32
ATGCCGCAACCACCATCTGGTGCGATGTGCGC
TACGGCGTTGGTGGTAGACCACGCTACACGCG
16
13
4
15
32
31
21
TCCAC TCGGC AGACC
AGGTG AGCCGTCTGG
GTAGAATCGCCTG
CATCTTAGCGGAC
CTCTGTATTGCCGAACTGG
GAGACAT AACGGCTTGACC
ACACTTACCTCTATGCGAACATCGGC TACTC
TGTGAATGGAGATACGCT TGTAGCCG ATGAG
GTGTCAGGCATCCTCGCTGT G
CACAGTCCGT AGGAGCGACAC
99
c
99
AGGTG AGCCGTCTGG
CATCTTAGCGGACGAGACAT AACGGCTTGACC
TGTGAATGGAGATACGCT TGTAGCCG ATGAG
CACAGTCCGT AGGAGCGACAC
TCCAC TCGGC AGACC
GTAGAATCGCCTGCTCTGTA TTGCCGAACTGG
ACACTTACCTCTATGCGAACATCGGC TACTC
GTGTCAGGCATCCTCGCTGT G
15
4
32
4
31
4
21
GGTTACCGCATAGGTC TA CCACCAACGCCGTA
CCAATGGCGTATCCAGAT G GTGGTTG CGGCAT
32
32
GCGCACATCGCACCAG
CGCGTGTAGCGTG
16
13
CGGCTGAACGCAGCAT
GCCGACTTGCGTC
16
13
GACCACGCTACACGCG
GTGCGATGTGCGC
16
13
TACGACGCAAGTCGGC
CTGCGTTCAGCCG
16
13
4
15
32
31
21
TCCAC TCGGC AGACC
AGGTG AGCCGTCTGG
GTAGAATCGCCTGCTCTGTA TTGCCGAACTGG
CATCTTAGCGGACGAGACAT AACGGCTTGACC
ACACTTACCTCTATGCGAACATCGGC TACTC
TGTGAATGGAGATACGCT TGTAGCCG ATGAG
GTGTCAGGCATCCTCGCTGT G
CACAGTCCGT AGGAGCGACAC
99

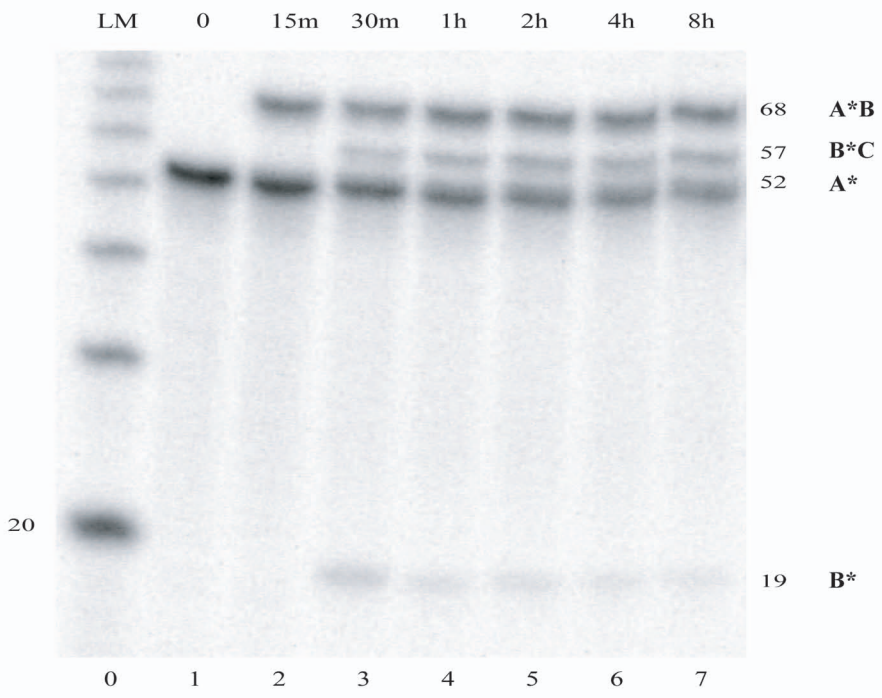
LM
0
15m
30m
1h
2h
4h
8h
68
A*B
57
B*C
52
A*
20
19
B*
0
1
2
3
4
5
6
7

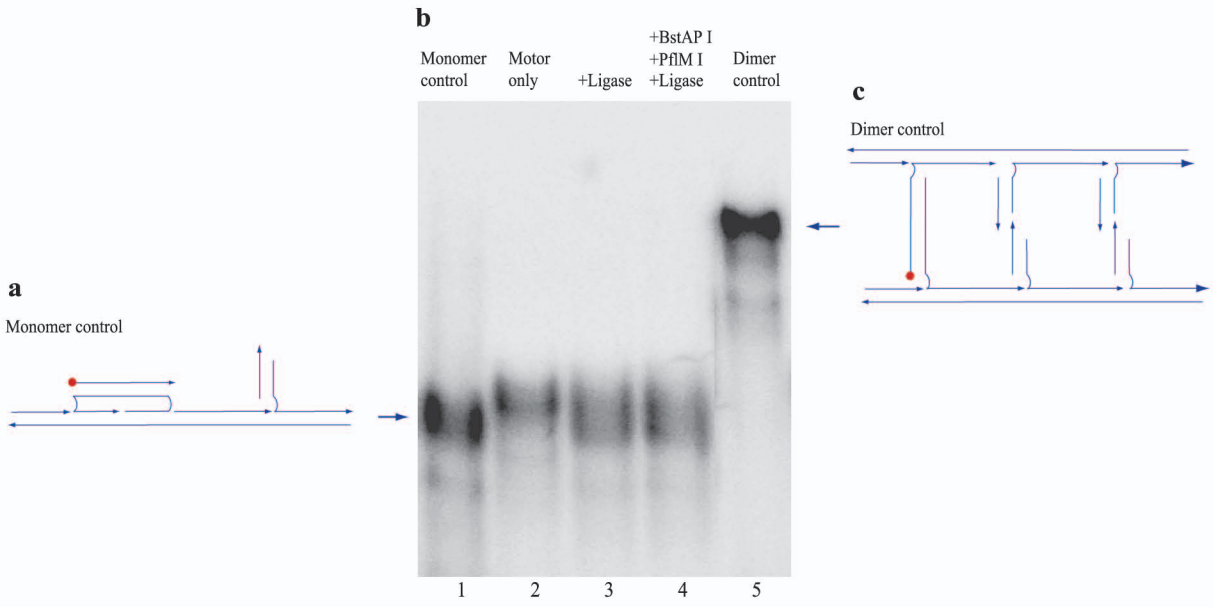
a
Monomer control
b
Monomer control
Motor only
+Ligase
+BstAP I +PflM I +Ligase
Dimer control
1
2
3
4
5
c
Dimer control